Application of a Transfer Function for Quick Estimation of Gas Flow Parameters – Useful Model-Based Approach for Enhance Measurements.

Mirosław Szukiewicz[1] and Adrian Szałek[1]

[1]Rzeszow University of Technology

May 5, 2020

Abstract

Applications of transfer function to derivation of a high precision model of tracer flow in a commercial measurement system is presented. A transfer function concept makes easier development of models of complex systems and consequently allows for obtaining a model that matches in the best way a physical system. The method has an additional profit viz. the same numerical algorithm i.e. inverse Laplace transform can be employed to solve the model both on the stage of precise model development (boundary value problem) and to find real model parameters (inverse boundary value problem). As a result of concept application, a very precise model of commercial measurement instrument was developed and, next, it was employed to determination of axial dispersion coefficients for empty tube and packed bed. Presented method is precise in wide range of operating conditions and faster comparing to other methods previously described in literature. The paper shows that mathematical modelling can be exploited to enhance measurements for a commercial measurement instrument i.e unlock the full potential of the commercial measurement system with no equipment design changes. The method is also a fast alternative to computational fluid dynamics for high precision calculations.

INTRODUCTION

The *transfer function* is a compact description of the input-output relation linear time invariant dynamical system. It provides information which specifies the behavior of the system, and is used in the mathematical analysis of systems. Transfer functions appear as relevant mathematical tools because they are usually easy for modification and easy for solution. They need only dynamics input–output data to represent even complex systems. One can say the transform function is "a black box" that transforms input into output signal. They can be applied to different systems however they are most often employed to estimate the response of dynamical systems and analysis of control systems. In the last field it was the primary tool used in classical control engineering. In the mentioned areas the concept of the transfer function is widely regarded as a powerful method of dealing with complex systems.

Mathematically the transfer function is a function of complex variables. It is obtained by inspection or by simple algebraic manipulations of the differential equations that describe the systems. The transfer functions can describe both simple one-dimensional systems and even infinite dimensional systems governed by partial differential equations. A complex model can be written very conveniently as an algebraic function of transfer functions of subsystems. The model reconstruction comes down to replacing one of the transfer function for subsystem by another one. Multiplication of transfer function and input function and, next, application of inverse Laplace transform algorithm results in the model solution.

Many textbooks provide a detailed account of transfer function derivation for simple, lumped parameters models. However chemical engineering employs mainly distributed parameters models for fluid flow and related processes description. Application of transfer function concept for the cases was limited due to problems with derivation of transfer function (differential equation should be solved) and with inverse Laplace transform (classical methods cannot be applied). In consequence few attempts have been made to investigate usefulness of the transfer function in chemistry, additionally the attempts mainly based on experimentally determined transfer functions what made possible to omit the mentioned problems. In the widely understood chemical engineering (without connections with control) there are really few published works. Kupper et al.[1] analyzed the problem of mass transport in discrete fracture networks. The authors developed a transfer function approach to mass transport modeling as a basis for comparing flowline routing or complete mixing models. The transfer function for the single fracture was derived from an analytical solution for a single fracture, while the intersection component was approximated by either the complete mixing or the streamline routing model. Different possible flow patterns at intersections were checked to develop an acceptable model. The results indicated that there is possible to develop a system analysis approach that could take the process of diffusion into matrix into account for complex, two-dimensional fracture networks. Marquez et al. [2] analyzed the heat processing of products immersed in a low-viscosity medium (the experiments were done with freshly harvested raspberries immersed in sucrose aqueous solution) where convection is the main heat transfer mechanism. The transfer function used in the paper had an assumed form (it was not a result of mathematical manipulations). Transfer function coefficients were calculated by simulating system evolution against a reference input signal. The authors concluded that the method approximates very well all practical situations of thermal treatment of raspberry preserves for the commoner systems, it gives the possibility of adjusting thermal treatments by allowing calculations and different sterilization policies can be easily tested to find that leading to maximum quality parameters. Sayyafzadeh et al.[3] proposed to use the transfer function to provide an accurate forecast of hydrocarbon reservoir performance during water flooding. They are proposed the method as a very good alternative of another methods: (i) a method that requires less data to simulate reservoirs but its outputs are not reliable in many cases, (ii) a complex, high accuracy method, that is time-consuming and requires large quantities of data. Different groups of transfer functions of subsystems were checked to develop a combination which has physical meaning and gives outputs with tolerable error. Four different cases were employed to validate the derived model. So, in this work, the transfer function concept was useful both for model development as well as simulations. Similarly, to the last reference transfer function coefficients were calculated based on experimental results. Kicsiny[4-5], Buzás and Kicsiny[6] as a way to improve solar collectors to get full solar systems efficiency as well as for better environmental protection indicated mathematical modeling with the use of system transfer functions. The transfer functions for solar heating systems with pipes were determined based on a validated mathematical model. The transfer functions were used for the dynamic analysis of a considered solar heating system. Effect of inlet temperature as well as initial temperature of collector were analyzed. The authors underline that the worked-out transfer functions are relatively easy to apply for dynamic analysis and stable control design. Ansorena and Di Scala[7], Glavina et al.[8-9], presented transfer function approach for food processing to estimate the thermal response of the system, e.g., to analyze the evolution of temperature in the geometrical center of potatoes during cooling and predict thermal histories of conductive foodstuffs. The authors applied simple mathematics to describe the processes behavior – only first or second order transfer functions however they obtained good approximations between predicted and experimental values. In the first paper the authors concluded that the model provides a very good approximation to experimental data and the main advantage of the transfer function is a much simpler mathematical model for parameter estimation. In the second one, they pointed that the model satisfactorily predicted the central temperature that is observed as a result of different forcing signals in the surrounding temperature. Moreover, the methodology could be applied to other fruits and vegetables and to different cooling or heating processes. And finally, in the last work authors analyzed both food and equipment thermal responses during cooking and retorting operations. The results were very satisfactory. The authors proposed this methodology as a potential approach to the implementation of new strategies leading to more efficient processes and to improve product quality. Application of transfer function makes easier developing a transient model and this property was explained the presented cases.

Since the above examples cover many various types of processes, therefore, it shows that the concept of transfer function is not limited to specific applications related to process control. However, the use of the transfer functions has one more practical aspect – it compels us to use inverse Laplace transform algorithms and, for more complex cases their numerical versions. Numerical algorithms of inverse Laplace transform are a topic with wide representation and many aspects. According to the literature reports, many scientists have been recommended numerical algorithms of inverse Laplace transform to find a solution in the time domain of a specific type of problem. Particular algorithms are suitable for various problems. A comprehensive review of earlier developed algorithms was presented by Davies and Martin [10]. Other studies on inversion methods based on precision of calculations and CPU time consumption are given by Wojcik et al [11] and Escobar et al [12].

Derivation and validation of a high precision model of tracer flow in a measurement system using transfer function is presented in this work. A transfer function concept makes easier to build and re-build models of complex systems and consequently allows for obtaining a model that matches in the best way a physical system. Transfer function for a system is based on theoretical model of gas flow. A system of partial differential equations is converted into a transfer function and next, a model solution is compared with the recorded outlet signal of a system. The mentioned above problems with transfer function derivation and solution of resulted Laplace domain model were minimized by application of CAS-type program, as described below. From an optimal fit of experimental and calculated signal curves dispersion coefficient is obtained. Details of the method is presented in Wojcik [13]. The method has an additional profit viz. - numerical inverse Laplace transform algorithm - can be employed for solution of a model. Transfer function models were solved using a relatively simple method i.e. numerical inverse Laplace transform algorithm presented by den Iseger [14]. Den Iseger method characterizes of a very broad scope for application; recently it is one the most often cited method in literature. The den Iseger's algorithm was coded by authors in Maple$^{(r)}$. Besides of computing of inverse Laplace transform, program Maple$^{(r)}$ was applied also for derivation of transfer functions (mathematical capabilities of program for analytic solutions of differential equation as well as integral transform were used). For the problem under consideration application of transfer function concept in combination with fast and precise algorithm and CAS-type computer program resulted in development of high precision mathematical model of the process and, consequently, determination of precise gas flow parameters. The method is very precise and it is faster comparing to methods previously described in literature.

Determination of dispersion coefficient is not mentioned as an application of the system used (Micromeritics' AutoChem 2950HP), so the method under consideration is the simple way with no equipment design changes and thus inexpensive technique to unlock the full potential of yours measurement system. Flexibility of the method is its large advantage – the model can be easily adjusted to other measurement system as well as modified to determining of other parameters e.g. effective diffusivity in the filled column etc. The method is a fast alternative to computational fluid dynamics for high precision calculations.

INSTRUMENT AND EXPERIMENT

The scheme of measuring system is presented in Figure 1.

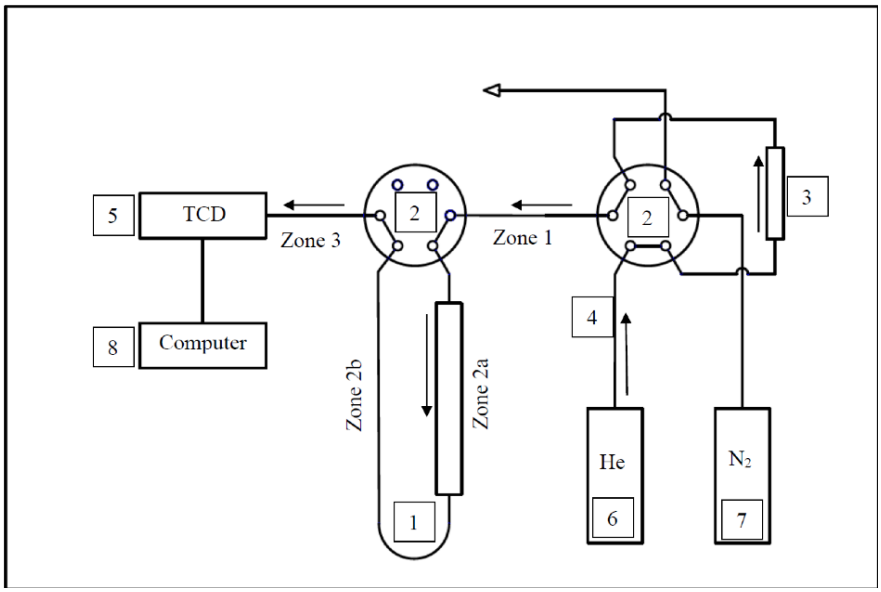

Fig. 1. Schematic diagram of the apparatus (Micromeritics' AutoChem 2950HP).

The measuring system consists of the following elements:

1. – an unit called by manufacturer the sample tube; the sample tube is U-shaped and consists of two elements that are inseparably connected, a front-end part of element with larger diameter is directly connected with the 6-way valve, similarly to tail-end part of element of smaller diameter; the element of larger diameter can work empty or it can be filled by catalyst, sorbent etc. (more information can be find on the manufacturer's website)
2. – the 6-way valve
3. – the sample loop
4. – steel pipes
5. –thermal conductivity detector (TCD)
6. – helium gas cylinder
7. – nitrogen gas cylinder
8. – computer.

The experiments were conducted in New Chemical Synthesis Institute, Pulawy (Poland) at each combination of the following process parameters:

- pressure: 2.00×10^5, 3.00×10^5 , Pa
- temperature: 313.15, 333.15, 353.15, K
- volumetric rate (at STP): 3.33×10^{-7} , 5.00×10^{-7} , m^3/s

The volume of sample loop was constant and equal to 2.50×10^{-7} m^3.

The system was flushed for 15-30 minutes with a constant flow of helium until a stable TCD signal was received. At the same time, the volume of sample loop was flushed also with a constant flow of nitrogen. Next, the 6-way valve was opened to allow the flow of helium with the constant volumetric flow rate through the system and the TCD signal was recorded.

In this study, experiments were carried out with the empty sample tube and with the packed sample tube. The sample tube was filled according to the Temkin's concept (Temkin and Kul'kova[15]), i.e., the sample tube was alternately filled with zinc oxide sorbent tablet PSC, with glass ball, again with zinc oxide sorbent tablets PSC, again with glass ball, etc. Sorbent tablets with average diameter and height of 4.8 mm, and

glass balls with average diameter of 5.1 mm were used. As a result, a bed of porosity e_e equal to 0,75 is obtained.

MODELS

In this section and the next one will be presented problems regarding derivation of a model that the best fits experiments. The proper choice of a model for the object is a complicated task. For the problem under consideration a model can be written very conveniently as a product of transfer functions of subsystems. The model reconstruction comes down to replacing one of the transfer functions for subsystem by another one. Multiplication of transfer function and input function (pulse) and, next, application of inverse Laplace transform algorithm results in the model solution. If few models are considered the presented procedure is simpler and faster than solution of set of partial differential equations.

Gas flow line through a system was divided into four zones (Fig. 1). The zones are distinguishable on the basis of geometry, function or both. Inner volume of the valves is neglected. Geometry of the apparatus was determined on the basis of technical data presented by manufacturer and previously made investigations [11, 13]. Table 1 gives a complete list of technical data.

Tab. 1. Flow zones description and data.

Number of the zone	Description of the zone	L_i [m]	$d_{w,i}$[m]
1	the pipe that connects the valves	20.0×10^{-3}	1.5875×10^{-3}
2a	sample tube – part of larger diameter	205.7×10^{-3}	7.6500×10^{-3}
2b	sample tube – part of smaller diameter	235.0×10^{-3}	1.5875×10^{-3}
3	the pipe that connects the valve to TCD detector	700.9×10^{-3}	1.5875×10^{-3}

An inlet concentration is given by (a rectangular signal pulse)

$$c_0 = \begin{cases} 0 & t < 0 \\ c_T & 0 \le t \le \frac{V_{\text{imp}}}{F_v} \\ 0 & t > \frac{V_{\text{imp}}}{F_v} \end{cases} \quad (1)$$

where: $c_T = \frac{P}{R_g \cdot T}$

Models are based on the following assumptions:

- the equation of state of an ideal gas describes the relationships for each of the gas components
- the system is operated under isothermal conditions.
- the pressure drop inside the channels is neglected (inner electronically controlled pressure regulator provide precise gas control)

Analysis of the gas flow line (Fig. 1) leads to the following conclusions:

- The valve dumps interactions of the zones 1 and 4 with zones 2a and zone 2b, respectively,
- the zones 2a and 2b interacts;

Interactions mentioned in the second bullet point can be treated as negligible, then the resulted mathematical model is much simpler for developing and easier for solution. They can also be treated as non-negligible, then the model derivation is a rather hard task. Since we could not safely accept a hypothesis on negligible interactions, we had to test two models. The first model, called further "model A", neglects interactions between zones 2a and 2b while the second one, "model B", takes them into account. The mass balance of nitrogen is presented by equation (2).

Mass balance equations.

$$\frac{\partial c(x,t)}{\partial t} = D_{L,i}\frac{\partial^2 c(x,t)}{\partial x^2} - \frac{F_v}{\varepsilon_e A_i} \bullet \frac{\partial c(x,t)}{\partial x} \qquad i = 1, 2a, 2b, 3 (2)$$

IC (for all zones)

$$c\,(x,0) = 0\ (3)$$

BC for Model A (interactions between zones 2a and 2b are not remarkable)

zone 1

$$F_v c\,(0^-,t) = F_v c\,(0^+,t) - A_1 D_{L,1}\ \left.\frac{\partial c(x,t)}{\partial x}\right|_{x=0^+} (4)$$

$$\left.\frac{\partial c(x,t)}{\partial x}\right|_{x=L_1^-} = 0 (5)$$

zone 2a

$$F_v c\left(L_1^-,t\right) = F_v c\left(L_1^+,t\right) - A_{2a} D_{L,2a}\ \left.\frac{\partial c(x,t)}{\partial x}\right|_{x=L_1^+} (6)$$

$$\left.\frac{\partial c(x,t)}{\partial x}\right|_{x=L_1+L_{2a}^-} = 0 (7)$$

zone 2b

$$F_v c\left(L_1+L_{2a}^-,t\right) = F_v c\left(L_1+L_{2a}^+,t\right) - A_{2b} D_{L,2b}\ \left.\frac{\partial c(x,t)}{\partial x}\right|_{x=L_1+L_{2a}^+} (8)$$

$$\left.\frac{\partial c(x,t)}{\partial x}\right|_{x=L_1+L_{2a}+L_{2b}^-} = 0 (9)$$

zone 3

$$F_v c\left(L_1+L_{2a}+L_{2b}^-,t\right) = F_v c\left(L_1+L_{2a}+L_{2b}^+,t\right) - A_3 D_{L,3}\ \left.\frac{\partial c(x,t)}{\partial x}\right|_{x=L_1+L_{2a}+L_{2b}^+} (10)$$

$$\left.\frac{\partial c(x,t)}{\partial x}\right|_{x=L_1+L_{2a}+L_{2b}+L_3} = 0 (11)$$

BC for Model B (interactions between zones 2a and 2b are remarkable)

Various boundary conditions on the border of the zone 2a and 2b is the difference between the models A and B. Presented here boundary conditions make allowance for interactions between the zones.

zone 2a + zone 2b

$$c\left(L_1+L_{2a}^-,t\right) = c\left(L_1+L_{2a}^+,t\right) (12)$$

$$F_v c\left(L_1+L_{2a}^-,t\right) - A_{2a} D_{L,2a}\ \left.\frac{\partial c(x,t)}{\partial x}\right|_{x=L_1+L_{2a}^-} = F_v c\left(L_1+L_{2a}^+,t\right) - A_{2b} D_{L,2b}\ \left.\frac{\partial c(x,t)}{\partial x}\right|_{x=L_1+L_{2a}^+} (13)$$

where

$$A_i = \frac{\pi d_i^2}{4} \qquad i = 1, 2a, 2b, 3 (14)$$

For empty zones $\varepsilon_e = 1$.

$c\ (L_{\ 1}+L_{\ 2a}+L_{\ 2b}+L_3,t\ )$, that is, the outlet concentration from the last zone corresponds to the signal recorded by the TCD-detector.

In both cases models consist of four partial differential equations with the initial and boundary conditions. Model A and B differ one to another in boundary conditions for zones 2a and 2b. This observation gave us an idea on how to improve and speed-up analysis of the problem. Numerical solution of the large system of equations, that may be stiff is rather tedious. We propose application of the transfer function concept. A transfer function is the ratio of an output variable to any input variable, in the Laplace domain. We choose outlet concentration from a zone as an outlet variable and, similarly, input concentration as an input variable.

In that case each zone is described by its own transfer function and, next, we can multiply the individual transfer function of each subsystem (zone) to obtain the overall transfer function. Model reconstruction is an easy task and, in practice, reduces to replacing a transfer functions for a subsystem by another one.

Illustrative example of development of transfer function

Development of transfer function will be presented for the zone 1. The mathematical model in real domain is presented by equation (2). In the first step, the governing equation with the boundary condition should be converted to the Laplace domain:

$sC + \frac{F_v}{A_1}\frac{\mathrm{dC}}{\mathrm{dx}} - D_{L,1}\frac{d^2C}{\mathrm{dx}^2} = 0 (15)$

BC for x=0

$F_v X = F_v \bullet C - A_1 D_{L,1}\frac{\mathrm{dC}}{\mathrm{dx}} (16)$

for x=L_1

$\frac{\mathrm{dC}}{\mathrm{dx}} = 0$ (17)

where:

capital letters describe the complex functions corresponding to the real functions,

X is the complex function that describe inlet concentration for the zone 1, i.e. $\mathcal{L}(c_0)$

and $w_2 = \frac{4F_v}{\pi d_{w,2}^2}$.

Integration to find a general solution and substitution of initial condition leads to

$C = K_1 e_1^x + K_2 e_2^x$ (18)

where

$r_1 = \sqrt{4A_1^2 D_{L,1} s + F_v^2}$ (19)

$e_1 = exp\left(\frac{(\mathrm{Fv}+r_1)}{2A_1 D_{L,1}}\right) (20)$

$e_2 = exp\left(\frac{(\mathrm{Fv}-r_1)}{2A_1 D_{L,1}}\right) (21)$

Constants of integration can be obtained from boundary conditions.

$K_1 = \frac{F_v X e_2^{L_1}\left(2A_1^2 D_{L,1} s + F_v^2 - F_v r_1\right)}{\left[\left(A_1^2 D_{L,1} s + \frac{F_v^2}{2} - \frac{F_v r_1}{2}\right)e_2^{L_1} - \left(A_1^2 D_{L,1} s + \frac{F_v^2}{2} + \frac{F_v r_1}{2}\right)e_1^{L_1}\right](F_v - r_1)} (22)$

$K_2 = \frac{F_v (F_v + r_1) X e_1^{L_1}}{\left(2A_1^2 D_{L,1} s + F_v^2 - F_v r_1\right)e_2^{L_1} - \left(2A_1^2 D_{L,1} s + F_v^2 + F_v r_1\right)e_1^{L_1}} (23)$

Substitution of integration constants and x=L_1 (zone outlet) to the general solution leads to outlet concentration. According to the definition, outlet concentration divided by inlet concentration (X) gives the transform function. After simplifications we obtain

$G_1(s) = \frac{C(L_1)}{X} = \frac{2F_v\left(r_1^2 - F_v r_1\right)e^{\frac{F_v L_1}{A_1 D_{L,1}}}}{(F_v - r_1)\left[\left(2A_1^2 D_{L,1} s + F_v^2 + F_v r_1\right)e_1^{L_1} - \left(2A_1^2 D_{L,1} s + F_v^2 - F_v r_1\right)e_2^{L_1}\right]} (24)$

Transfer functions for the other zones can be obtained in the same way.

The overall transfer function of a system can be easily obtained by multiplication of transfer functions of the zones 1..3:

$$G(s) = G_1(s) \bullet G_{2a}(s) \bullet G_{2b}(s) \bullet G_3(s) = \frac{C|_{x=L_1}}{C_0(s)} \frac{C|_{x=L_1+L_{2a}}}{C|_{x=L_1}} \frac{C|_{x=L_1+L_{2a}+L_{2b}}}{C|_{x=L_1+L_{2a}}} \frac{C|_{x=L_1+L_{2a}+L_{2b}+L_3}}{C|_{x=L_1+L_{2a}+L_{2b}}} = \frac{C|_{x=L_1+L_{2a}+L_{2b}+L_3}}{C_0(s)} \quad (25)$$

Multiplication by C_0 and application of inverse Laplace transform gives outlet concentration from the system that is concentration recorded by TCD

$$c|_{x=L_1+L_{2a}+L_{2b}+L_3} = \mathcal{L}^{-1}(G(s) \bullet c_0(s)) \quad (26)$$

All calculations were carried out using Maple®2017. den Iseger algorithm was used for finding inverse Laplace transform of right-hand side of above equation. Precision of the algorithm is high (see Appendix 1). Since numerical inverse Laplace transform is not supported by Maple, the implementation of den Iseger algorithm was coded by the authors. Determination of D_L-value requires application of optimization methods (the inverse boundary value problem). The build-in global optimization procedure of Maple (GlobalSolve) was used. The aim function was based on areas ratio of experimental and calculated signal curves (factor f presented in the Tables below is a reflection of the areas ratio; f=1 corresponds to the perfect fit). From an optimal fit of experimental and calculated signal curves we get D_L-value.

RESULTS AND DISCUSSION

Experiments were conducted in two regimes:

- the sample tube was empty
- the sample tube was packed

Empty sample tube

Typical results for Model A and Model B are presented in Fig 2 and Table 2 for empty sample tube. In the figures we present comparison of experimental (solid line) and calculated (circles) signal curves for both models for few experiments. In the tables we present values of dispersion coefficient as well as f-values for all experiments.

In the Fig. 2 we present results of simulations obtained for model A (left panel) and for model B (right panel) for the same operating conditions. More experimental results are presented in Table 2. For model A in the Fig. 2a (Experiment No. E4) we observe good, then in Fig. 2b (Experiment No. E7) average and in Fig. 2c (Experiment No. E12) rather poor fit. Poor fits for model B are not observed. We can conclude that in this case interactions between zone 2a and zone 2b are significant. f-values ranged between 0.921 and 0.962 for the Model A and between 0.973 and 0.993 for Model B and the observation justifies presented conclusion. The best fits for Model A correspond to the worse for Model B.

Let's trace how D_L-values varies with temperature and pressure for both models. In addition to D_L-values there are also presented products of multiplying of D_L by pressure and by temperature raised to the -3/2 power. This product should have a constant value, and, it actually is almost constant both for Model A and B with one exception. Result of experiment E1 seems to be an outlying result. Dixon's Q-test confirmed this supposition for both models and the result was discarded. Statistics of remaining results are included in Table 2. The first and most important conclusion drawn is that small values of standard deviation and the confidence interval justified correctness of the method of identification of dispersion coefficient. It is easily to observe that standard deviation and confidence interval for Model B are about 40% smaller than for Model A. It additionally indicates that D_L coefficients should be evaluated using model B. This conclusion is important – average percentage difference between D_L-values determined from model A and from model B reach 15 percent. So, in the case of empty tube, model B can be recommended as more precise than model A.

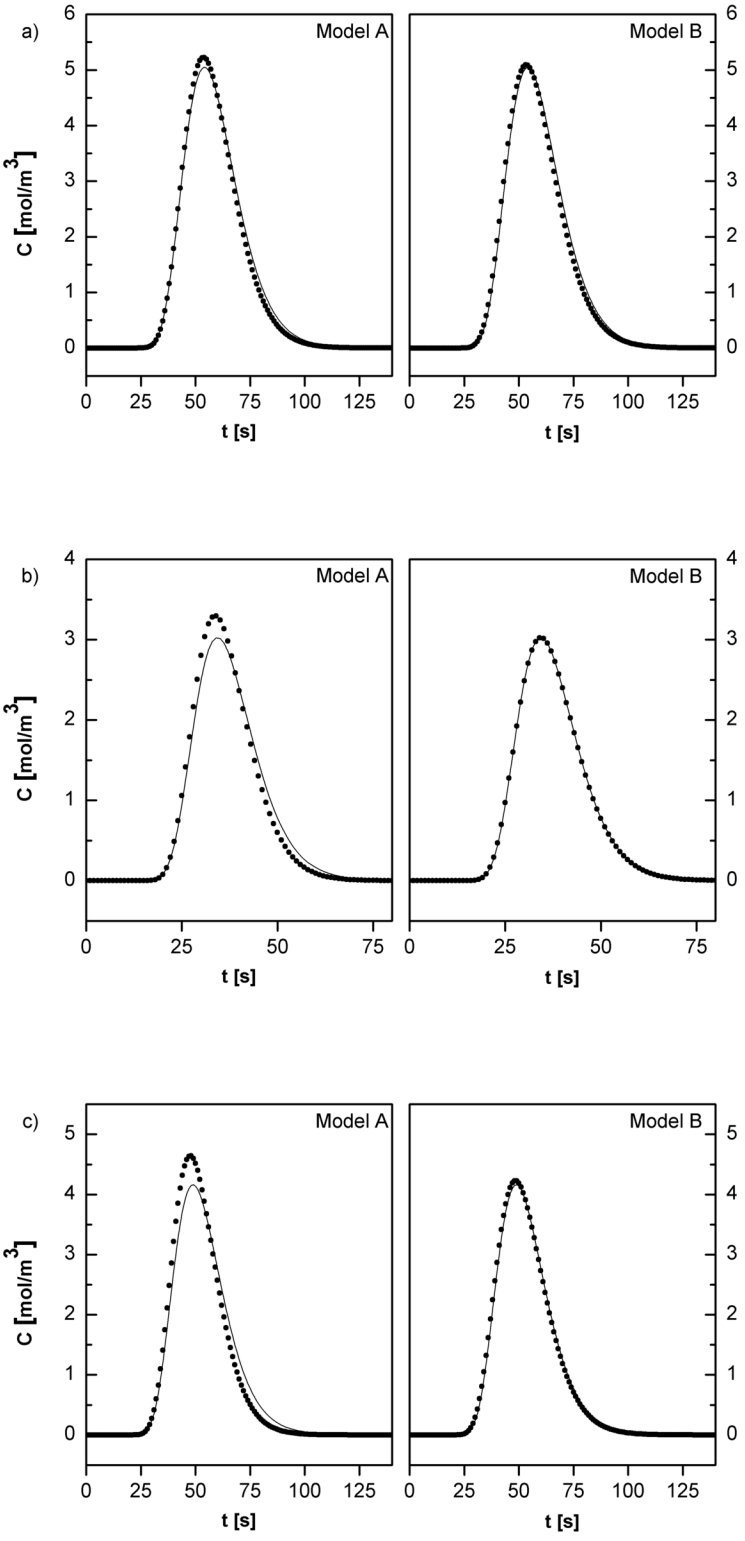

Fig. 2. Results of Model A and Model B solutions for non-packed sample tube; solid line – experiment, *

calculations; a) T=313 K, p=3.00×10^5 Pa, F_v=5.00×10^{-7} m^3/s; b) T=333 K, p=2.00×10^5 Pa, Fv=5.00×10^{-7} m^3/s; c) T=353 K, p=3.00×10^5 Pa, F_v=5.00×10^{-7} m^3/s

Table 2. Results of Model A and Model B solutions for non-packed sample tube

Exp. No.	T [K]	$F_v\times10^7$ [m^3/s]	P [MPa]	**Model** A $D_L\times10^5$ [m^2/s]	**Model** A f [-]	**Model** A $D_L PT^{-3/2}\times10^3$	**Model** B $D_L\times10^5$ [m^2/s]	**Model** B f [-]	**M** B D_L $\times1$
P1	313	3.33	0.2	3.64	0.9843	1.314	3.64	0.9852	1.3
P2			0.3	2.23	0.9901	1.207	2.23	0.9911	1.2
P3		5.00	0.2	3.92	0.9930	1.415	3.92	0.9930	1.4
P4			0.3	**2.47**	**0.9709**	**1.337**	**2.54**	**0.9862**	**1.3**
P5	333	3.33	0.2	3.94	0.9921	1.296	3.96	0.9940	1.3
P6			0.3	2.48	0.9833	1.224	2.50	0.9862	1.2
P7		5.00	0.2	**4.26**	**0.9921**	**1.401**	**4.28**	**0.9921**	**1.4**
P8			0.3	2.69	0.9737	1.327	2.70	0.9766	1.3
P9	353	3.33	0.2	4.22	0.9930	1.272	4.23	0.9930	1.2
P10			0.3	*3.62*	*0.9872*	*1.636*	*3.64*	*0.9891*	*1.6*
P11		5.00	0.2	3.63	0.9872	1.094	3.71	0.9901	1.1
P12			0.3	**2.69**	**0.9823**	**1.216**	**2.80**	**0.9843**	**1.2**
						1.282	mean value	mean value	1.2
						0.093	standard deviation	standard deviation	0.0
						0.063	confidence interval	confidence interval	0.0

Experiments presented in Fig.2 are marked bold. Outlying result is underlined.

Packed sample tube

Analogous experiments were carried out for packed sample tube. In Fig. 3 and Table 3 are presented results. In opposition to empty tube there is no visible differences in results obtained using Model A and B. Evaluated values of dispersion coefficient are almost the same. Only detailed analysis can yield more specific results for model B f-values are slightly closer to unity and standard deviation and confidence interval are slightly smaller than for model A (similarly to the preceding section one outlying result was discarded). So, the model B is more precise than model A but for packed tube the difference is rather without practical meaning. A bed inside the Zone 2 efficiently damps interactions between Zones 2 and 3 and application of more complex model do not bring more accurate results, differences are about 1%. It is noteworthy that small values of standard deviation and the confidence interval justified correctness of the method of identification of dispersion coefficient for packed bed as well.

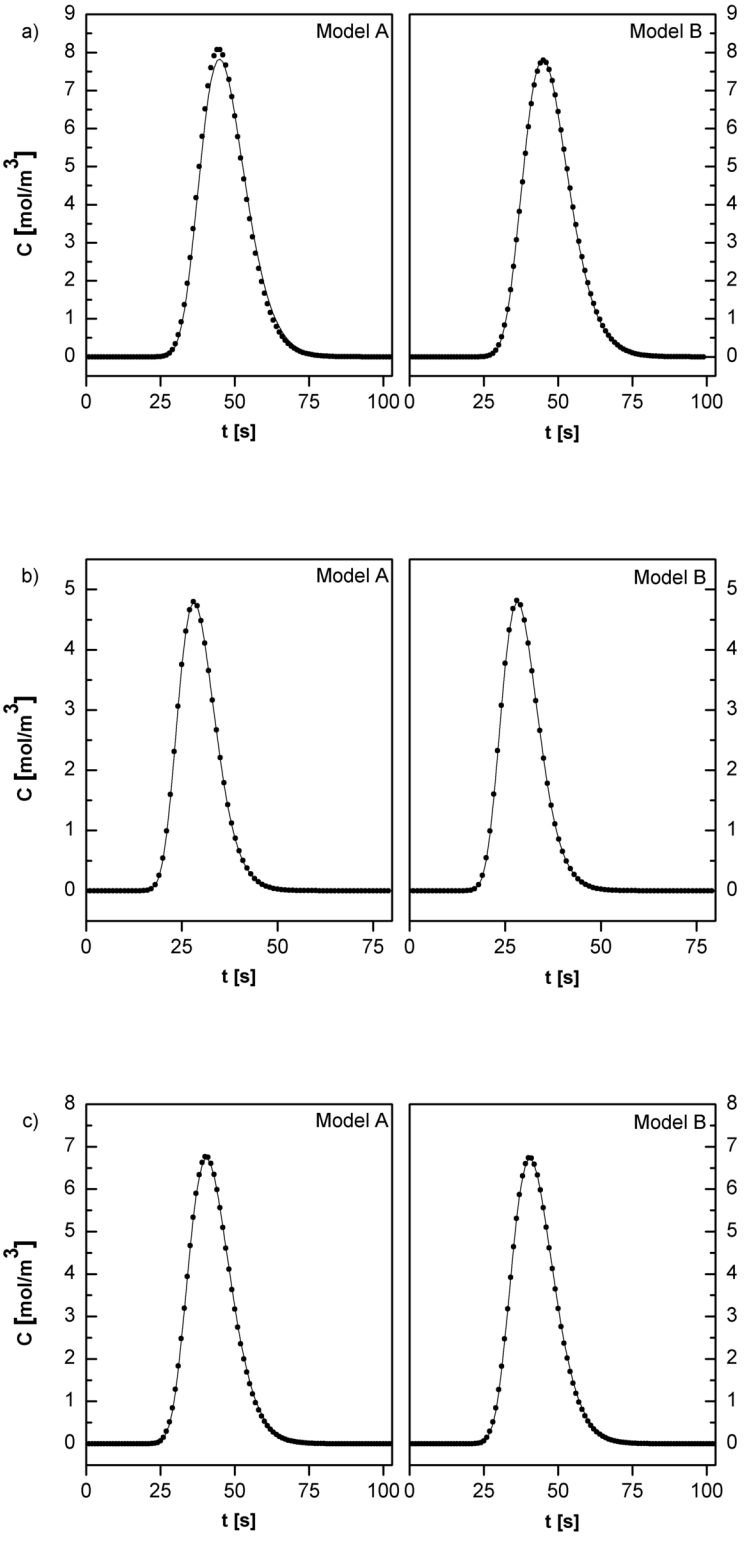

Fig. 3. Results of Model A and Model B solutions for packed sample tube; solid line – experiment, *

calculations; a) T=313K, p=3.00×10^5 Pa, F_v=5,00×10^{-7} m^3/s; b) T=333 K, p=2.00×10^5 Pa, F_v=5.00×10^{-7} m^3/s; c) T=353 K, p=3.00×10^5 Pa, F_v=5.00×10^{-7} m^3/s

Tab 3. Results of Model A and Model B solutions for packed sample tube.

Experiments presented in Fig.3 are marked bold. Outlying result is underlined (it was detected as in the Section A).

Both for non-packed and packed sample tube, the values of axial dispersion coefficients (the Peclet numbers values are of several tens) indicate that the flow is neither plug flow nor perfect mixing under operation conditions applied. It is rather unexpected result for the packed vessel, the literature [15] indicates a high probability of plug flow.

The results show that the transfer function and inverse Laplace transform are very effective technique for solution of the model. It helps in easier way to develop model of high precision. In the Appendix 2 we discuss results obtained for the same experiment and CFD model of gas flow. The results presented show that transfer function-based model fits the experiments better - deviations and confidence interval are few times smaller. So, the models based on transfer function can be recommended as the alternative for models coded using CFD programs.

Summarizing, the method discussed can be recommended to determine of gas flow and axial dispersion coefficients. It should be pointed that the method is fast. Excluding operation condition stabilization time, the total time of measurement and calculations is in the order of minutes (less than 15 minutes).

CONCLUSIONS

On the basis of calculations performed the following conclusions can be drawn:

- Application of the concept of transfer function is a very effective technique to develop precise version of the model. Properties of transfer functions help to examine many model versions and to ensure choice of the best one.
- Interactions between elements of the empty sample tube strongly influence results and the more complex model B is recommended; model A is of less precision.
- If the first element of sample tube includes a bed, interactions between elements are strongly reduced and simpler model A can be recommended; model B is of comparable precision to model A.
- In all cases, very good fit between numeric and experiment curves were obtained.
- den Iseger algorithm ensures fast calculations of good precision and can be recommended for application; the algorithm is a very effective for distributed parameters systems.
- The method presented is a quick procedure to determine of gas flow parameters and it is faster comparing to other methods previously described in literature. It can be an alternative for using CFD programs.
- The Computer Algebra System (CAS) - Maple(r) is very helpful for fast and error free derivation of very complex transfer functions for distributed parameters models.

ACKNOWLEDGEMENTS

The authors would like to thank Researches from New Chemical Synthesis Institute in Pulawy (Poland) for sharing the experimental data.

CONFLICT OF INTEREST

Authors have no conflict of interest relevant to this article.

NOMENCLATURE

$c(L_i, t)$ outlet concentration of tracer$\left(mol \bullet m^{-3}\right)$

$\acute{c}(L_i, s)$ solution of model for zone in Laplace domain, $i = 1 \ldots 3$

c_0 inlet concentration of tracer$\left(mol \bullet m^{-3}\right)$

$D_{L,i}$ axial dispersion coefficient in *i-th*zone$(m^2 \bullet s^{-1})$, $i = 1 \ldots 3$

$d_{w,i}$ diameter of the zone $(m\ )$, $i = 1 \ldots 3$

F_v volumetric flow rate $(m^3 \bullet s^{-1})$,

$G_i\,(s)$ transfer function for zone, $i = 1 \ldots 3$

$G\,(s)$ transfer function for system

L_i length of *i-th* zone $(m\ )$, $i = 1 \ldots 3$

P pressure $(Pa\ )$

R_g universal gas constant $(J \bullet \mathrm{mol}^{-1} \bullet K^{-1})$

s Laplace transform parameter

T temperature $(K\ )$

t time of calculations $(s\ )$

V_{imp} volume of sample loop $(m^3\ )$

Greek symbols

ε_e bed porosity

REFERENCES

1. J.A. Kupper, F.W. Schwartz, P.M. Steffler, A comparison of fracture mixing models, 1. A transfer function approach to mass transport modeling, J. Contam. Hydrol., 1995, 18, 1-5. https://doi.org/10.1016/0169-7722(94)00044-I
2. C.A. Marquez, A. De Michelis, V.O. Salvadori, R.H. Mascheroni, Application of Transfer Functions to the Thermal Processing of Particulate Foods Enclosed in Liquid Medium, J. Food Eng., 1998, 38, 189-204.
3. M. Sayyafzadeh, P. Pourafshary, M. Haghighi, F. Rashidi, Application of transfer functions to model water injection in hydrocarbon reservoir, J. Petrol. Sci. Eng., 2011, 78, 139-148. https://doi.org/10.1016/j.petrol.2011.05.009
4. R. Kicsiny, Transfer functions of solar heating systems with pipes for dynamic analysis and control design, Solar Energy, 2017, 150, 596-605. https://doi.org/10.1016/j.solener.2017.05.006
5. R. Kicsiny, Transfer functions of solar heating systems for dynamic analysis and control design, Renew. Energy, 2015, 77, 64-76. https://doi.org/10.1016/j.renene.2014.12.001
6. J. Buzas, R. Kicsiny, Transfer functions of solar collectors for dynamical analysis and control design, Renew. Energy, 2014, 68, 146-155. https://doi.org/10.1016/j.renene.2014.01.037
7. M.R. Ansorena, K.C. Di Scala, Predicting thermal response of conductive foods during start-up of process equipment using transfer functions, J. Food Eng., 2010, 33, 168-175. DOI: 10.1111/j.1745-4530.2008.00343.x
8. M.Y. Glavina, K.C. Di Scala, R. Ansorena, C.E. del Valle, Effect of dimensions on the cooling rate of whole potatoes applying transfer functions, LWT-Food Sci. Technol., 2007, 40, 1694-1697. https://doi.org/10.1016/j.lwt.2007.03.012
9. M. Glavina, K. Di Scala, C. Del Valle, Estimation of thermal diffusivity of foods using transfer functions, LWT-Food Sci. Technol., 2006, 39, 455-459. https://doi.org/10.1016/j.lwt.2005.03.010
10. B.Davies, B. Martin. Numerical inversion of the Laplace transform: A survey and comparison of methods., J. Comput. Phys., 1979, 33:1-32. DOI: 10.1016/0021-9991(79)90025-1

11. M. Wojcik, M. Szukiewicz, P. Kowalik, Application of Numerical Laplace Inversion Methods in Chemical Engineering with Maple(r), Journal of Applied Computer Science Methods, 2015, 7, 5-15. https://doi.org/10.1515/jacsm-2015-0006
12. F.H. Escobar, F.A. Leguizamo, J.H. Cantillo, Comparison of Stehfest's and Iseger's algorithms for Laplacian inversion in pressure well tests. J. Eng. Appl. Sci., 2014, 9(6), 919-922.
13. M. Wojcik, Zastosowanie przekształcenia Laplace'a do badania nieustalonych procesów dyfuzyjno-dyspersyjnych, (Application of Laplace transform to analysis of diffusion/dispersion for unsteady-state processes), PhD Thesis, Rzeszow, 2018.
14. P. Den Iseger, Probab. Numerical Transform Inversion Using Gaussian Quadrature, Eng. Inf. Sci., 2006, 20, 1-43. https://doi.org/10.1017/S0269964806060013
15. M.I. Temkin, N.V. Kul'kova, Лабораторный Реактор Идеалного Вытеснения, Kinetics and Catalysis, 1969, 10, 461-463.

Appendix A.

Tests for accuracy of den Iseger's algorithm

To ensure usefulness for the considered problem of den Iseger's algorithm as well as its precision we made tests for the following test functions:

$y(s) = \frac{1}{s^2+s+1}$ (A1)

$y(s) = \frac{2 \bullet s}{(s^2+1)^2}$ (A2)

$y(s) = \frac{1}{\sqrt{s}+\sqrt{s+1}}$ (A3)

$y(s) = \frac{1}{4} \frac{25 \bullet sinh(4 \bullet \sqrt{\frac{s}{2}})}{sinh(5\sqrt{\frac{s}{2}}) \bullet s}$(A4)

Corresponding to them functions in time domain are given by eq. (A5)-(A8):

$y(t) = \frac{2}{3} \bullet \sqrt{3} \bullet exp(-\frac{1}{2} \bullet \sqrt{3} \bullet t) \bullet sin(\frac{1}{2} \bullet \sqrt{3} \bullet t)$(A5)

$y(t) = t \bullet \sin(t)$ (A6)

$y(t) = \frac{1-exp(-t)}{\sqrt{4 \bullet \pi \bullet t^3}}$(A7)

$y(t) = 5 + \frac{50}{4\pi} \bullet \sum_{n=1}^{\infty} \left(\frac{(-1)^n}{n} \bullet \sin\left(\frac{4n \bullet \pi}{5}\right) \bullet \exp\left(\frac{2n^2 \bullet \pi^2}{25} \bullet t\right)\right)$(A8)

A comment is required for equations (A4) and (A8). Eq. (A4) is a Laplace domain solution the following diffusion equation:

$\frac{\partial C(r,t)}{\partial t} = a \bullet \frac{1}{r^2} \frac{\partial}{\partial r}(r^2 \bullet \frac{\partial C(r,t)}{\partial r})$(A9)

with appropriate initial and boundary conditions

$C(r,0) = 0$ (A10)

$\frac{\partial C(r,t)}{\partial r}|_{r=0} = 0$ (A11)

$C(r = R, t) = C_0$ (A12)

Analytic solution of the presented initial-boundary value problem is as follows:

$C(r,t) = C_0 + \frac{2 \bullet R \bullet C_0}{\pi \bullet r} \bullet \sum_{n=1}^{\infty} \left(\frac{(-1)^n}{n} \bullet \sin\left(\frac{n \bullet \pi \bullet r}{R}\right) \bullet \exp\left(\frac{n^2 \bullet \pi^2}{R^2} \bullet a \bullet t\right)\right)$(A13)

It is easily to check that eq.(A8) for a=2, R=5, C0=5 and r=4 corresponds to eq.(A13)

The tests were carried out for two different time steps $\frac{t_m}{N}$ (N=32 or N=128). Results are presented in Table A1.

Table A1. Standard deviation between numerical and analytic solutions and relative time of computations

Test function	Standard deviation N=32	Standard deviation t_{32} [-]	Standard deviation N=128	Standard deviation t_{128} [-]
eq.(A1)	1.08×10^{-12}	1	1.07×10^{-13}	21.3
eq.(A2)	3.30×10^{-14}	1	3.72×10^{-14}	20.2
eq.(A3)	2.74×10^{-7}	1	2.17×10^{-7}	13.7
eq.(A4)	2.48×10^{-12}	1	9.8×10^{-15}	3.7

In all cases precision of calculation was good or very good. Reduction of the time step increases precision of calculations but time required for computations increases too.

Summarizing the tests performed, den Iseger algorithms can be employed to calculation presented in the main part of the article.

Appendix B.

Comparison of results for model B and for CFD model.

Results obtained from model B and model CFD coded in Comsol package were compared as previously described in RESULTS AND DISCUSSION section. Results are presented in Table B1 and in Fig. B1. The dispersion coefficients values are similar, the average difference is about five percent. However statistical indicators presented in Table B1 show that the method based on transfer function (model B) fits experimental result better than CFD model. The same relation is visible in Fig. B1, as well. Lines that are generated by model B lies closer to the experimental lines than those generated by model CFD. It confirm the conclusion formulated in the main part of the paper, that models based on transfer function can be recommended as the alternative for models coded using CFD programs.

Table B1. Results of Model B and Model CFD solutions for non-packed sample tube

Exp. No.	T [K]	$F_v\times10^7$ [m^3/s]	P [MPa]	**Model** B $D_L\times10^5$ [m^2/s]	**Model** B $D_L PT^{-3/2}\times10^3$	**Model** CFD $D_L\times10^5$ [m^2/s]	**Model** CFD $D_L PT^{-3/2}\times10^3$
E2	313	3.33	0.3	3.33	1.803	3.41	1.847
E3		5.00	0.2	4.88	1.761	4.69	1.694
E4			0.3	**3.26**	**1.765**	**3.36**	**1.820**
E5	333	3.33	0.2	5.29	1.740	5.77	1.899
E6			0.3	3.49	1.722	3.53	1.743
E7		5.00	0.2	**5.19**	**1.707**	**5.75**	**1.892**
E8			0.3	3.49	1.722	3.83	1.891
E9	353	3.33	0.2	5.70	1.718	5.25	1.583
E10			0.3	3.76	1.700	3.62	1.637
E11		5.00	0.2	5.59	1.684	5.90	1.779
E12			0.3	**3.78**	**1.709**	**3.50**	**1.583**
					1.730	mean value	1.760
					0.034	standard deviation	0.122
					0.023	confidence interval	0.082

Experiments presented in Fig.B1 are marked bold. Outlying result is removed.

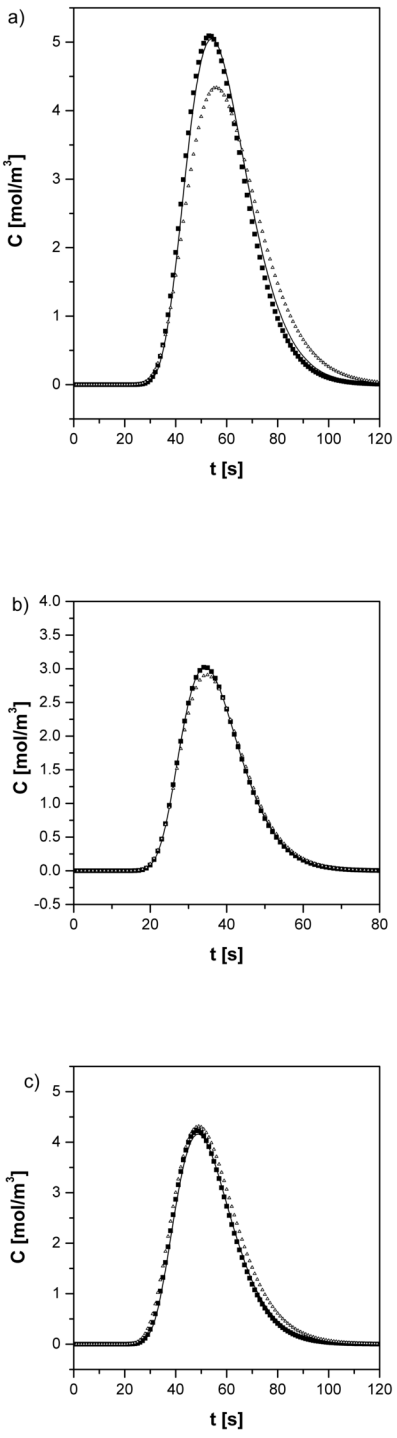

Fig. B1. Results of Model B and Model CFD solutions for non-packed sample tube; solid line – experiment, model B, $^{m}odelCFD; a) T = 313K, p = 3.0010^{5} Pa, F_{\mathrm{v}} = 5.0010^{-7} m^{3}/s; b) T = 333K, p = 2.0010^{5} Pa, F_{\mathrm{v}} =$

$5.0010^{-7} m^3/s; c) T = 353K, p = 3.0010^5 Pa, F_{\mathrm{v}} = 5.0010^{-7} m^3/s$